Direct dynamics simulations of photoexcited charge-transfer-to-solvent states of the $I^-(H_2O)_n$ (n = 4, 5 and 6) clusters

Kenta Takahashi, Toshiyuki Takayanagi*

Department of Chemistry, Saitama University, 255 Shimo-Okubo, Sakura-ku, Saitama City, Saitama 338-8570, Japan

Abstract

The dynamics of photoexcited charge-transfer-to-solvent (CTTS) states of the $I^-(H_2O)_n$ (n = 4, 5 and 6) clusters has been studied using the on-the-fly direct dynamics technique in order to understand recent femtosecond pump-probe experiments from a theoretical viewpoint. The lowest triplet potential energy surface at the hybrid B3LYP density-functional electronic structure level was employed to model the CTTS singlet excited-state potential energy surface due to small singlet-triplet splittings. A total of 13 structures of the $I^-(H_2O)_n$ cluster were vertically excited with the initial kinetic energy being zero and subsequent trajectory simulations were performed up to 1.5-2.0 ps. It was found that features of time-evolution of vertical detachment energy of an excess electron and dipole moment along the trajectory is strongly dependent of the initial cluster structure employed. The simulations revealed that the structural change in the water network configuration due to breaking of hydrogen-bonds plays an important role in the dynamics. I-atom detachment from the cluster was not observed during simulation time but this result is presumably due to the too strong attractive interaction between I and H_2O on the B3LYP potential energy surface.

Corresponding author. *E-mail address*: tako@chem.saitama-u.ac.jp (T. Takayanagi)

1. Introduction

It is well-known that solvated electrons or hydrated electrons play a very important role in various chemical and biological processes in solutions [1,2]. In particular, they play a key role in DNA damage processes induced by radiation [3]. Understanding of early stage dynamics of such processes has been an important issue in various fields including chemistry, physics and biology. Although electron solvation phenomena are intrinsically condensed phase ones, previous experimental studies clearly show that molecular clusters are quite useful for understanding the structure, dynamics and reactivity of solvated electrons from a microscopic point of view [4-8]. This is because clusters can easily be generated under gas phase conditions and then various sophisticated spectroscopic and time-resolved techniques can be applied to such clusters. Needless to say, water anion clusters $(H_2O)_n^-$ have been most extensively studied in the past from both experimental and theoretical sides.

It is generally accepted that $I^-(H_2O)_n$ iodide-anion water clusters are very good systems for understanding the production and relaxation dynamics of excess electrons by solvent molecules since photoexcitation of these systems to the so-called charge-transfer-to-solvent (CTTS) band, in which the strongly bound excess electron in the iodide is ejected into the surrounding solvent molecules, leads to efficient production of excess electrons in the clusters [9]. Neumark and co-workers [10-14] have carried out extensive experimental work on the dynamics of the CTTS excitation of the $I^-(H_2O)_n$ clusters using a sophisticated femtosecond pump-probe photoelectron spectroscopic technique. They have measured time-evolution of the vertical detachment energy (VDE) of the excess electron in clusters by systematically varying cluster size. For $I^-(H_2O)_3$ and $I^-(H_2O)_4$ clusters, VDE was found to increase only slightly with simple population decay of the excited-states. They have interpreted this result to mean that autodetachment of the excess electron occurs before the I atom leaves the cluster. On the other hand, for larger clusters with $n \geq 5$, the observed time-resolved spectra showed that the VDE of the excited cluster increased by 0.1-0.4 eV within several hundred femotoseconds ~ 1 picoseconds. This finding was

interpreted in terms of stabilization of the ejected excess electron through rearrangement of solvent molecules. This model also accounts for the observed isotope effects exhibiting a difference in the time-evolution of the VDE between $I^-(H_2O)_n$ and $I^-(D_2O)_n$ clusters.

Subsequently, Chen and Sheu [15,16] proposed that the experimentally observed VDE increase is due to the neutral I atom detachment from the cluster on the basis of 'static' ab initio quantum-chemical calculations, where the solvent moiety was frozen in the same configuration as in the original $I^-(H_2O)_n$ cluster. Notice that this interpretation is therefore conflict with the interpretation of Neumark et al.[10-12] A similar theoretical interpretation has also been reported by Kim and co-workers [17]. They have suggested that the neutral I atom is readily released from the cluster upon photoexcitation to the CTTS excited state.

It should be emphasized that dynamics calculations would be very informative for understanding the experimental results of Neumark et al from a theoretical point view. Recently, Timerghazin and Peslherbe [18] and Kołaski et al. [19] have independently performed trajectory simulations after CTTS photoexcitation to the excited-state potential energy surface using a direct dynamics computational technique. These two groups have employed the complete-active-space self-consistent (CASSCF) approach to obtain the excited-state potential surfaces. Since the CASSCF calculations are generally time-consuming, their calculations were limited to a very small system of $I^-(H_2O)_3$. Interestingly, they have observed rapid rearrangements of water molecules and relatively slow I-atom detachment from the cluster in their dynamics calculations; however, these two groups have given somewhat different conclusions. Timerghazin and Peslherbe [18] concluded that both iodine and solvent motions must be taken into account to fully rationalize experimental observations since time-evolutions of the VDE may be affected by the present of the neutral I atom. On the other hand, by comparing the dynamics of $I^-(H_2O)_3$ to that of $Cl^-(H_2O)_3$ and $(H_2O)_3^-$ clusters, Kołaski et al. [19] have concluded that the role of the halide atom is not significant in the solvent rearrangement process except for very early processes where the excited electron density initially induces the detachment of the iodide atom.

Unfortunately, Kołaski et al. did not discuss the effect of the I atom on the time-evolution of the VDE in detail.

Motivated by the current status on theoretical investigation as mentioned above, we have recently carried out direct dynamics simulations of the CTTS photoexcitation process for the $I^-(H_2O)_6$ cluster [20]. We have employed the lowest triplet potential energy surface since we have found that the features of the lowest singlet excited-state potential surface are quite similar to those of the lowest triplet surface. We have reported preliminary calculations for two book-type structures of $I^-(H_2O)_6$ cluster. In this paper, we report full accounts of our previous work and present direct dynamics simulations for the $I^-(H_2O)_4$, $I^-(H_2O)_5$ and $I^-(H_2O)_6$ clusters.

2. Computational Method

We have performed direct dynamics calculations to simulate the CTTS photoexcitation dynamics of the $I^-(H_2O)_n$ (n = 4-6) clusters on the lowest triplet potential energy surface [20,21]. The BOMD (Born-Oppenheimer Molecular Dynamics) method, implemented in the GAUSSIAN03 program package [22], was used for all calculations. This method uses a fifth-order polynomial fitted to the energy, gradient, and Hessian at each time step, and then the step size was taken to be much larger than the step size used in the normal method utilizing only the gradient information [23].

Most of calculations were done with the hybrid density-functional unrestricted B3LYP level [24,25], but a part of the calculations was carried out with the BLYP and BHLYP functionals in order to understand the effect of exchange-correlation functionals on the BOMD dynamics. The BHLYP method, a variant of Beck's "half and half" function, has been employed since a previous study of Herbest and Head-Gordon [26,27] shows that this method gives reliable VDE values for water cluster anions. The basis sets used in the present study were chosen to be small to save computational time. However, it is generally known that diffuse functions are necessary to describe

the very diffuse nature of the excess electron distribution. We have applied the recent strategy proposed by Herbest and Head-Gordon [26,27], who have performed systematic ab initio as well as density-functional theory (DFT) calculations for water cluster anions. We employed the 6-31(1+,3+)G* basis sets, where two additional diffuse *s*-orbitals are added on the original 6-31+G* basis set of hydrogen atoms while the standard 6-31+G* basis set is used for O atoms. The exponents are scaled values of the outermost s-shell of the 6-31+G* basis set of hydrogen with a progression factor being 1/3. In their more recent study [27], the progression factor of 1/3.32 has been employed. Since we have found that these two basis sets give very similar dynamics, their original factor of 1/3 was employed. For an iodine atom, a Stuttgart-Dresden quasi-relativistic ECP46MWB effective core potential [28] was used, but additional diffuse functions were not augmented. However, as will be shown in later, additional diffuse functions and polarization functions [29] were added in the potential energy profile calculations as well as VDE calculations by the CASPT2 and MRCI methods. Notice that these CASPT2 and MRCI calculations were performed in order to confirm the accuracy of the DFT calculations. In all cases of n = 4-6, eight electrons were distributed among the I-5*sp* orbitals and the dipole-bound orbital for obtaining the CASSCF reference wave function. These multi-configurational calculations were performed using the MOLPRO program [30].

In this work, we have chosen several low-lying energy clusters as an initial structure of the BOMD calculation. We set the initial kinetic energies of the system to zero. This is a somewhat unrealistic condition although the previous dynamics simulations for the $I^-(H_2O)_n$ cluster [18,19] have also been made with zero kinetic energy. It is possible to apply finite kinetic energy (finite cluster temperature); however, it may be difficult to choose appropriate initial conditions. Presumably, many trajectories should be integrated if we use the finite temperature condition; such calculations are beyond our computational costs.

The structures of the $I^-(H_2O)_n$ (n = 4-6) clusters in the ground electronic state have been previously and extensively studied by an initio method as well as density functional method in the past. It is now understood that the geometric structures of the

$I^-(H_2O)_n$ clusters are largely determined by a combination of the interaction between the I^- anion and the dipole moment of water network and hydrogen-bond interaction between I^- and the dangling hydrogen atoms. The most extensive work has been carried out by Lee and Kim [31], who reports many structures and energetics of the ground-state $I^-(H_2O)_n$ clusters. The structures of the $I^-(H_2O)_n$ clusters employed in this work are summarized in Fig. 1. Notations of the $I^-(H_2O)_n$ clusters are exactly the same as those used in the paper of Lee and Kim [31]. For n = 4, we have chosen C4 and C1' conformers since these two structures are reported to be more stable than other conformers. The C4 cluster is the most stable form and has a four-membered cyclic structure with C_4 symmetry, where I^- is supported by four dangling hydrogen atoms and the cluster has four hydrogen bonds. The C1' is the second lowest form, where I^- is supported by two water molecules in the three-membered cyclic structure and one branched water. In the case of n = 5, we have chosen Y41, R43, Y41', and Y32 conformers. Among these conformers, the Y41 cluster is reported to be most stable. For n = 6, we have chosen Bd, Bd', Bf, Bf', Bgf, R6 and Y42 conformers. It should be important to mention that all the $I^-(H_2O)_n$ clusters employed in this study can be classified as surface-type clusters, where I^- is located on the surface of the water clusters. Lee and Kim [31] have previously found that the $I^-(H_2O)_n$ systems have some minima, for which I^- is internally solvated inside of the water clusters. However, such structures are reported to be less stable than the surface-type clusters at least for small size clusters (n = 4-6).

3. Results and Discussion

Before presenting results of the BOMD simulations, it is important to demonstrate the validity to use the lowest triplet potential energy surface as a model of the singlet CTTS excited-state potential energy surface [32]. Fig. 2 compares the potential energy profiles calculated at various levels of theory for the C4 $I^-(H_2O)_4$ cluster. As mentioned previously, the ground-state $I^-(H_2O)_4$ cluster in the most stable

form has a four-membered cyclic structure with C_4 symmetry. In Fig. 2, the potential energy profiles are plotted as a function of the dihedral angle between the 'crown' H atoms and the plane formed by the four O atoms. First, it is seen that the MRCI potential energy curve for the lowest CTTS singlet state is very similar to that for the lowest triplet state. This clearly indicates that the singlet-triplet splitting is quite small at least for the $I^-(H_2O)_4$ cluster although spin-orbit interaction is not taken into account in the present calculation. It is seen that both singlet and triplet potential energy curves of the CTTS states are strongly repulsive along the dihedral angle in the vertical excitation region. Fig. 2 also shows the lowest triplet potential energy curves obtained at the B3LYP, BLYP and BHLYP levels of theory. It is noticed that these triplet potential energy curves are similar in character to the MRCI potential energy curves. This is quite encouraging since this agreement suggests that the dynamics calculations on the potential energy surface at the DFT level of theory may be similar to those on a more accurate MRCI potential energy surface of the CTTS singlet excited state. We have also calculated the potential energy curves at the CASPT2 level of theory. Essentially the same result as the MRCI one was obtained although detailed curves are not shown.

We have further confirmed the magnitude of the singlet-triplet energy splittings for the larger $I^-(H_2O)_5$ and $I^-(H_2O)_6$ clusters. We have carried out single-point MRCI calculations at the ground-state optimized structures. As a result, it was found that that the lowest triplet state is slightly stable than the lowest singlet excited-state and that the corresponding energy splitting is in the range of 0.014-0.063 eV. This result implies the validity to use the triplet potential energy surface in the dynamics also for the larger $I^-(H_2O)_5$ and $I^-(H_2O)_6$ clusters.

Fig. 3 compares DFT potential energy profiles for the hydrogen-bonding interaction between two H_2O molecules and for the interaction between I and H_2O. It is expected that these potential energy curves play a crucial role in the photoexcitation dynamics, as will be described below. For the hydrogen-bonding interaction between two water molecules, it is seen that all the B3LYP, BLYP and BHLYP methods yield a very similar result, as shown in Fig. 3, but the BHLYP method gives a somewhat

deeper potential well. The previous CCSD(T) calculations [33] with large basis sets yielded the dissociation energy of the water dimer to be 0.22 eV. Although the DFT results give somewhat larger dissociation energies than the CCSD(T) data, the agreement seems to be reasonable.

Figs. 3b and 3c show the potential energy curves for I-H_2O as a function of the I-O distance and I-H distance, respectively, within Cs symmetry constraint but for two different configurations. A previous CCSD(T) study of Kowal et al. [34] indicates that the energetically lowest structure is characterized by the direct O-I bond with Cs symmetry. Thus, the CCSD(T) result fairly agrees with the DFT result. However, the well depth is somewhat dependent of exchange-correlation functionals used in the DFT method. The BLYP method gives the deepest well of 0.24 eV, while the BHLYP method gives the most shallow well of 0.16 eV. Since the previous CCSD(T) calculation [34] gives the I-OH_2 binding energy to be 0.108 eV, it is probable that these DFT binding energies may be too large. For the I-H hydrogen bond, the binding energy obtained at the CCSD(T) level was estimated to be 0.052 eV. It is seen from Fig. 3c that the BLYP calculation gives a comparable result to the CCSD(T) result, while the binding energies obtained at the B3LYP and BHLYP levels are somewhat smaller than the BLYP result.

Now let us present results of dynamics calculations. Fig. 4 displays the time evolution of the total kinetic energy, total electronic energy (potential energy), dipole moment, and VDE for the photoexcited C4 $I^-(H_2O)_4$ cluster obtained from the BOMD simulation at the B3LYP level of theory. The dipole moment and VDE values were obtained from the same level B3LYP calculations of the neutral doublet state for the geometry at each BOMD time step. The corresponding structural changes are presented in Fig. 5 along with the changes of electron density of the highest occupied molecular orbital (HOMO). After photoexcitation, the "dangling" hydrogen atoms, which initially form H-I^- hydrogen bonds in the ground-state, suddenly move away from the iodide atom. Then, the structure of the water cluster becomes flat and is then inverted at t = 97 fs. After this, a flat structure was again seen for the water cluster moiety at t = 259 fs. This structural change is essentially the same as that seen in the

previous dynamics calculation for the $I^-(H_2O)_3$ cluster of Timerghazin and Peslherbe [18]. It is seen that the four-membered structure retains during about ~ 1000 fs although the I atom is bound to the O atom in a water molecule. One hydrogen bond is subsequently broken and the cyclic structure is thus deformed at t ~ 1175 fs. Notice that the cyclic structure of water network finally converted into a linear chain structure at t ~ 1500 fs. This process is quite similar to the results of Timerghazin and Peslherbe [18] and of Kołaski et al [19]. However, a completely different dynamics was obtained for the iodide atom motion. Timerghazin and Peslherbe [18] have found that the heavy iodide atom was slowly departing from the $(H_2O)_3^-$ anion cluster although the energy partitioned into the iodide kinetic energy was found to be very small (~ 0.01 eV). Kołaski et al. [19] also found the iodide detachment dynamics in their simulation, where the kinetic energy of the I atom were estimated to be 0.03-0.04 eV. On the other hand, in our BOMD simulation, the iodide atom does not detach from the water cluster but is finally bound to the terminal water molecule in the linear chain $(H_2O)_4^-$ cluster. This difference in the dynamics is presumably due to the difference in the I-H_2O potential energy between the B3LYP and CASSCF electronic structure methods. As presented in Fig. 3, the B3LYP method gives a somewhat large binding energy between I and H_2O. Presumably, the CASSCF binding energy for the I-H_2O interaction may be much smaller than the DFT value since it is often pointed out that the CASSCF method underestimates long-range dispersion interaction due to the lack of the dynamical electron correlation effect.

It is interesting to note that the dipole moment and the VDE value increase with an increase in time along the calculated trajectory, as is shown in Fig. 4. However, these two curves are not parallel as a function of time. This means that the magnitude of VDE does not exclusively determined only by the magnitude of the overall dipole moment of the corresponding neutral configuration of the water cluster. The slight increase in the VDE value is in qualitative agreement with the result of the femtosecond experiment. However, it has been previously pointed out by Herbert and Head-Gordon [26,27] that the hybrid B3LYP level calculations generally give large VDE values for $(H_2O)_n^-$ clusters. This suggests that the present B3LYP/6-31(1+,3+)G* method also

yields too large VDE values for the $I^-(H_2O)_n$ cluster system. In order to confirm this, we have additionally carried out the MRCI and CASPT2 calculations using geometries along the BOMD trajectory obtained at the B3LYP/6-31(1+,3+)G* level. The result of the MRCI calculations are also plotted in Figs. 4c and 4d. The essentially the same result was obtained for the CASPT2 calculation. For the dipole moment, agreement between the B3LYP and MRCI(CASPT2) results was found to be excellent. On the other hand, as for the VDE value, the B3LYP method significantly overestimates its absolute value, as expected. However, it is encouraging that the B3LYP and MRCI VDE curves show a very similar trend as a function of time.

Fig. 6 shows the results of the BOMD simulation for the C4 $I^-(H_2O)_4$ cluster at the BLYP and BHLYP levels of theory. We have found that the BLYP method show very similar dynamics to the B3LYP result. One hydrogen bond was broken and a linear type cluster was obtained. We can also see the increase in the VDE and dipole moment with the increase in time similar to the B3LYP result. In the case of the BHLYP functional, a somewhat different dynamics was obtained as shown in Fig. 6. In this case, the four-membered cyclic structure was not broken and the water network structure remains the same as the initial structure although the I atom is bound to the O atom in one water molecule. This difference is presumably due to the somewhat deep hydrogen-bonding well of the BHLYP potential (see Fig. 3). This suggests that the small difference in the potential energy surface slightly alter the feature of the relaxation dynamics of the photoexcited $I^-(H_2O)_n$ cluster. However, it should be emphasized that a large number of trajectories should be integrated in order to understand the source of the difference more quantitatively. In the following, we will present results of the BOMD simulation obtained at the B3LYP level of theory.

The results of the BOMD simulation of the photoexcited Y41' $I^-(H_2O)_5$ cluster are presented in Figs. 7 and 8. Fig. 7 shows an analogous plot of Fig. 4 while the snapshots of selected configurations along the trajectory are displayed in Fig. 8. Similar to the results of C4 $I^-(H_2O)_4$ cluster, a linear type structure was finally obtained in the calculated trajectory ($t \sim 1500$ fs). Also, a gradual increase of the VDE value is seen with the increase in time. However, the change in the dipole moment as a

function of time is somewhat different from the VDE change. Interestingly, the VDE value obtained at the B3LYP level of theory is quite similar to that obtained at the MRCI level.

Fig. 9 shows the time evolution of the total kinetic energy, total electronic energy, (potential energy), dipole moment, and vertical detachment energy for the photoexcited Bf-type $I^-(H_2O)_6$ cluster. The corresponding structural changes along the trajectory are presented in Fig. 10. A sudden decrease in the potential energy is seen just after photoexcitation; however, change in the potential energy after this is not so significant. On the contrary, it is interesting to note that the dipole moment gradually increases with the increase in time. This is due to water network rearrangement from the book-type structure to linear-type structure. The excess electron is initially localized around the one dangling hydrogen atom. It is interesting to note that the strong repulsive force between the excess electron and the I atom is playing an important role in an early stage of this trajectory. The excess electron is always localized around the original position and the I atom is readily departing from the excess electron moiety. The book-type structure in the Bf confirmer is subsequently destroyed accompanying breaking of some hydrogen bonds. This suggests the repulsive force between I and an excess electron is strong enough to break hydrogen bonds. However, since the corresponding repulsive energy is not larger than the I-O attractive interaction, the I atom is still bound to the terminal water molecule. It is seen that the linear-type structure is formed in this trajectory and that the excess electron is strongly bound to the terminal water molecule.

It is seen from Fig. 9 that agreement between the B3LYP and MRCI results is found to be excellent for the dipole moment value. On the other hand, it is found that the VDE value obtained at the B3LYP method is larger than the MRCI result. However, we should notice that the difference in the VDE value between the B3LYP and MRCI results is nearly constant and the corresponding value is seen to be about 0.2 eV. In fact, it can be seen that the VDE curve obtained at the B3LYP level is almost parallel to that obtained at the MRCI level. This comparison thus implies that we can qualitatively discuss the time evolutions of the VDE value even at the B3LYP level of

theory.

Fig. 11 summarizes time-evolutions of the VDE and dipole moments values obtained for all BOMD simulations examined in this study. Table 1 also summarizes structures obtained in the present simulations (t = 1.5-2.0 ps). In all cases, an increase in the VDE value is seen with an increase in time except for the Y32, Bd, Bd', Bgf and Y42 structures. For these five initial structures, it is seen that the change in the VDE and dipole moment is not so significant. Therefore, we have to conclude that the VDE change is strongly dependent of the initial structure of the $I^-(H_2O)_n$ cluster. In addition, the present BOMD simulations show that the VDE change in the range of $0 < t <$ 1.5-2 ps is exclusively due to the structural change in the water network in clusters. Needless to say, breaking of hydrogen-bond as well as cyclic structure and the location of the excess electron play an essential role in determining the water structural change and the VDE change. Table 1 shows that linear structures are mainly formed in the present simulation (1.5-2.0 ps). Notice that structures obtained in the trajectory calculations are not always the most stable forms. We have carried out 1.5-2.0 ps trajectory calculations and this propagation time is still too short that the calculated trajectory cannot sample all of phase space. We believe that the trajectories obtained in this work show only initial processes of photoexcitation. The observed structural change is presumably due to the combination of the repulsive force between the I atom and e^- (on the excited-state surface) and attractive force between I and O in H_2O.

We did not observe the detachment of the I atom from the cluster during our simulation time of 1.5-2 ps. This result may be due to fact that the attractive force between the I atom and O atom in H_2O is somewhat stronger than more accurate CCSD(T) result. Recent experimental study of Kammrath et al. [12] reports that the I-atom loss occurs prior to autodetachment for clusters with $n > 5$. However, it should be emphasized that the present theoretical calculations are not in contradictory to their experimental study. Kammrath et al. [12] have concluded that the I atom loss occurs on a very slower time scale. For example, the time constant of the I-atom detachment for the $I^-(H_2O)_6$ cluster has been estimated to be about 38 ps, which is much longer than the present simulation time. Thus, it may take much longer time that an excess energy

is partitioned into the I-atom detachment mode even for the small $I^-(H_2O)_n$ (n = 4-6) clusters.

4. Summary and future directions

In order to understand recent femtosecond pump-probe experiments of Neumark et al. [10-14] from a theoretical viewpoint, we have performed direct dynamics simulations of photoexcitation to the CTTS excited state of the $I^-(H_2O)_n$ (n = 4, 5, and 6) cluster anions. The simulations were done on the lowest triplet potential energy surface as a model of the singlet CTTS excited-state surface. The on-the-fly dynamics simulations were performed at the B3LYP hybrid density-functional level of theory, which was determined from the comparison of the excited-state potential energy curves to more accurate MRCI potential energy curves. A total of 13 cluster configurations were chosen as initial structures of the photo-excitation simulations. We have obtained time evolutions of the geometrical rearrangement in the cluster as well as the vertical detachment energy of an excess electron and the overall dipole moment along the classical trajectory. It was found that the VDE change and dipole moment change strongly depend on the initial cluster structure and thus depends on the subsequent structural change in the water network in the cluster. The I-atom detachment from the cluster was not observed during our simulation time. Although our result is significantly different from previous calculations on the $I^-(H_2O)_3$ cluster obtained at the CASSCF level of theory [18,19], the difference is presumably due to the difference of the I-H_2O interaction potential between the CASSCF and density-functional methods. We have noticed that the B3LYP method gives a too deep attractive potential well for the I-H_2O interaction.

Although the present simulations have already provided an important insight into the relaxation dynamics of photoexcited $I^-(H_2O)_n$ clusters, it should be emphasized that a large number of trajectories taking the structural fluctuation effect into account should be done in order to make a quantitative connection with the femtosecond

pump-probe experiments. Due to computational costs, an efficient sampling scheme for initial conditions would be an important next step in the future simulations. It should be mentioned that the present dynamical simulation does not include neither electronically nonadiabatic effects [2] nor electron detachment processes since the dynamics calculations were made on the lowest adiabatic potential energy surface in the triplet state. As shown in Fig. 2, three singlet (or triplet) potential energy surfaces are very close in energy. This suggests that electronically nonadiabatic transitions between these states may play some roles in the photoexcitation dynamics. Also, the inclusion of the internal conversion to the ground state via electronically nonadiabatic transitions is an interesting future subject. In addition, there is a possibility that quantum tunneling may play a significant role in dynamics of hydrogen-bond rearrangement processes. In spite of these limitations, we believe that the present photoexcitation simulation is a good starting point for future theoretical studies.

Acknowledgement

This work was partly supported by the Grant-in-Aid for Scientific Research of the Ministry of Education, Culture, Sports, Science, and Technology of Japan (Grant No. 17550007).

References

[1] E. J. Hart, M. Anbar, The Hydrated Electron (Wiley-Interscience, NewYork, 1970).

[2] P. J. Rossky, J. Schnitker, J. Phys. Chem. 92 (1988) 4277.

[3] C. von Sonntag, The Chemical Basis of Radiation Biology (Taylor and Francis, London, 1987).

[4] J. V. Coe, G. H. Lee, J. G. Eaton, S. T. Arnord, H. W. Sarkas, K. H. Bowen. L. Ludewigt, H. Haberland, D. R. Worsnop, J. Chem. Phys. 92 (1990) 3980.

[5] G. H. Lee, S. T. Arnord, J. G. Eaton, H. W. Sarkas, K. H. Bowen, C. Ludewigt, H. Haberland, Z. Phys. D 20 (1991) 9.

[6] N. I. Hammer, J. W. Shin, J. M. Headrick, E. G. Diken, J. R. Roscioli, G. H. Weddle, M. A. Johnson, Science 306 (2004) 675.

[7] A. E. Bragg, J. R. R. Verlet, A. Kammrath, O. Cheshnovsky, D. M. Neumark, Science 306 (2004) 669.

[8] D. H. Paik, I. Lee, D. Yang, J. S. Baskin, A. H. Zewail, Science 306 (2004) 672.

[9] D. Serxner, C. E. H. Dessent, M. A. Johnson, J. Chem. Phys. 105 (1996) 7231.

[10] L. Lehr, M. T. Zanni, C. Frischkorn, R. Weinkauf, D. M. Neumark, Science 284 (1999) 635.

[11] A. V. Davis, M. T. Zanni, R. Weinkauf, D. M. Neumark, Chem. Phys. Lett. 353 (2002) 455.

[12] A. Kammrath, J. R. R. Verlet, A. E. Bragg, G. B. Griffin, D. M. Neumark, J. Phys. Chem. A 109 (2005) 11475.

[13] J. R. R. Verlet, A. Kammrath, G. Griffin, D. M. Neumark, J. Chem. Phys. 123 (2005) 231102.

[14] D. E. Szpunar, K. E. Kautzman, A. E. Faulhaber, D. M. Neumark, J. Chem. Phys. 124 (2006) 054318.

[15] H.-Y. Chen, W.-S. Sheu, Chem. Phys. Lett. 335 (2001) 475.

[16] H.-Y. Chen, W.-S. Sheu, Chem. Phys. Lett. 353 (2002) 459.

[17] H. M. Lee, S. B. Suh, K. S. Kim, J. Chem. Phys. 119 (2003) 7685.

[18] Q. K. Timerghazin, G. H. Peslherbe, J. Am. Chem. Soc. 125 (2003) 9904.

[19] M. Kołaski, H. M. Lee, C. Pak, M. Dupuis, K. S. Kim, J. Phys. Chem. A 109 (2005) 9419.

[20] T. Takayanagi, K. Takahashi, Chem. Phys. Lett. 431 (2006) 28.

[21] T. Takayanagi, J. Phys. Chem. A110 (2006) 7011.

[22] Gaussian 03, Revision B.04, M. J. Frisch et. al, Gaussian, Inc., Pittsburgh PA, 2003.

[23] J. M. Millam, V. Bakken, W. Chen, W. L. Hase, B. H. Schlegel, J. Chem. Phys. 111 (1999) 3800.

[24] A. D. Becke, J. Chem. Phys. 98 (1993) 5648.

[25] C. Lee, W. Yang, R. G. Parr, Phys. Rev. B 37 (1988) 785.

[26] J. M. Herbert, M. Head-Gordon, J. Phys. Chem. A 109 (2005) 5217.

[27] J. M. Herbert, M. Head-Gordon, Phys. Chem. Chem. Phys. 8 (2006) 68.

[28] A. Bergner, M. Dolg, W. Kuechle, H. Stoll, H. Preuss, Mol. Phys. 80 (1993) 1431

[29] M. N. Glukhovtsev, A. Pross, M. P. McGrath, L. J. Radom, J. Chem. Phys. 103 (1995) 1878.

[30] MOLPRO, a package of ab initio programs, H.-J. Werner and P. J. Knowles, version 2002.1, R. D. Amos, A. Bernhardsson, A. Berning, P. Celani, D. L. Cooper, M. J. O. Deegan, A. J. Dobbyn, F. Eckert, C. Hampel, G. Hetzer, P. J. Knowles, T. Korona, R. Lindh, A. W. Lloyd, S. J. McNicholas, F. R. Manby, W. Meyer, M. E. Mura, A. Nicklass, P. Palmieri, R. Pitzer, G. Rauhut, M. Schütz, U. Schumann, H. Stoll, A. J. Stone, R. Tarroni, T. Thorsteinsson, and H.-J. Werner.

[31] H. M. Lee, K. S. Kim, J. Chem. Phys. 114 (2001) 4461.

[32] F. D. Villa, K. D. Jordan, J. Phys. Chem. A 106 (2002) 1391.

[33] W. Klopper, J. G. C. M. van Dujineveldt-van de Rijdt, F. B. van Duijeneveldt, Phys. Chem. Chem. Phys. 2 (2000) 2227.

[34] M. Kowal, R. W. Gora, S. Roszak, J. Leszczynski, J. Chem. Phys. 115 (2001) 9260.

Table 1. Summary of BOMD calculations

Initial Structure	Approximate structure obtained at t ~ 1.5-2.0 ps
$I^-(H_2O)_4$	
C4 (4[a])	$I^-\cdots(H_2O)_4$ (3[a], 4-*linear*[b])
C4 (4) (BLYP)	$I^-\cdots(H_2O)_4$ (3, 4-*linear*)
C4 (4) (BHLYP)	$I^-\cdots(H_2O)_4$ (3, 4-*cyclic*)
C1' (4)	$I^-\cdots(H_2O)_4$ (4, 3-*cyclic*+1-*branch*[c])
$I^-(H_2O)_5$	
Y41' (5)	$I^-\cdots(H_2O)_5$ (5, 5-*linear*)
R43 (6)	$I^-\cdots(H_2O)_5$ (5, 4-*cyclic*+1-*branch*)
Y41 (5)	$I^-\cdots(H_2O)_5$ (6, 5-*cyclic*)
Y32 (5)	$I^-\cdots(H_2O)_5$ (5, 3-*cyclic*+2-*branch*)
$I^-(H_2O)_6$	
Bf (7)	$I^-\cdots(H_2O)_6$ (5, 6-*linear)*
Bf' (7)	$I^-\cdots(H_2O)_6$ (7, 6-*cyclic*)
Bd (7)	$I^-\cdots(H_2O)_6$ (6, 4-*cyclic+2-branch*)
Bd' (7)	$I^-\cdots(H_2O)_6$ (7, 6-*cyclic*)
Bgf (7)	$I^-\cdots(H_2O)_6$ (5, 6-*linear*)
Y42 (7)	$I^-\cdots(H_2O)_6$ (6, 4-*cyclic+2-branch*)
R6 (6)	$I^-\cdots(H_2O)_6$ (6, 5-*cyclic+1-branch*)

[a]Numbers in parentheses are corresponding to the number of water-water hydrogen bonds.

[b]"*m-linear*" means a linear-type cluster structure consisting of *m* water molecules.

[c]"*m-cyclic*+*n-branch*" means that the cluster has a cyclic structure consisting of *m* water molecules with branched *n* water molecules.

Figure Captions

Fig. 1 Geometric structures of $I^-(H_2O)_n$ (n = 4, 5, and 6) clusters. Notations (Y: Branched hydrogen-bonding, R: ring, B: book, d: dipole-driven structure, f: free two dangling H atoms) have been taken from the paper of Ref. 31 to distinguish the structures.

Fig. 2 Potential energy curves for the $I^-(H_2O)_4$ cluster as a function of the dihedral angle θ. The upper panel shows potential curves for the electronically excited-states while lower panel for the ground state.

Fig. 3 Potential energy curves for the hydrogen-bonding interaction between two H_2O molecules and for the interaction between I and H_2O

Fig. 4 Time evolutions of the total kinetic energy (a), total electronic energy (b), dipole moment (c), and vertical detachment energy (d) along the trajectory of the photoexcited C4 $I^-(H_2O)_4$ cluster.

Fig. 5 Snapshots of selected configurations along the trajectory of the photoexcited C4 $I^-(H_2O)_4$ cluster. The O-H hydrogen bonds and I-H bonds are drawn using dotted lines and dashed lines, respectively. The excess electron density plots are also shown.

Fig. 6 Time evolutions of vertical detachment energy and dipole moment obtained from the BOMD simulations at the (a) BLYP and (b) BHLYP levels of theory. Selected snapshots are also shown.

Fig. 7 Same as Fig. 4 but for the Y41' $I^-(H_2O)_5$ cluster.

Fig. 8 Same as Fig. 5 but for the Y41' $I^-(H_2O)_5$ cluster.

Fig. 9 Same as Fig. 4 but for the Bf $I^-(H_2O)_6$ cluster.

Fig. 10 Same as Fig. 5 but for the Bf $I^-(H_2O)_6$ cluster.

Fig. 11 Time evolutions of vertical detachment energy and dipole moment obtained for all $I^-(H_2O)_n$ (n = 4, 5 and 6) initial structures examined in this work.

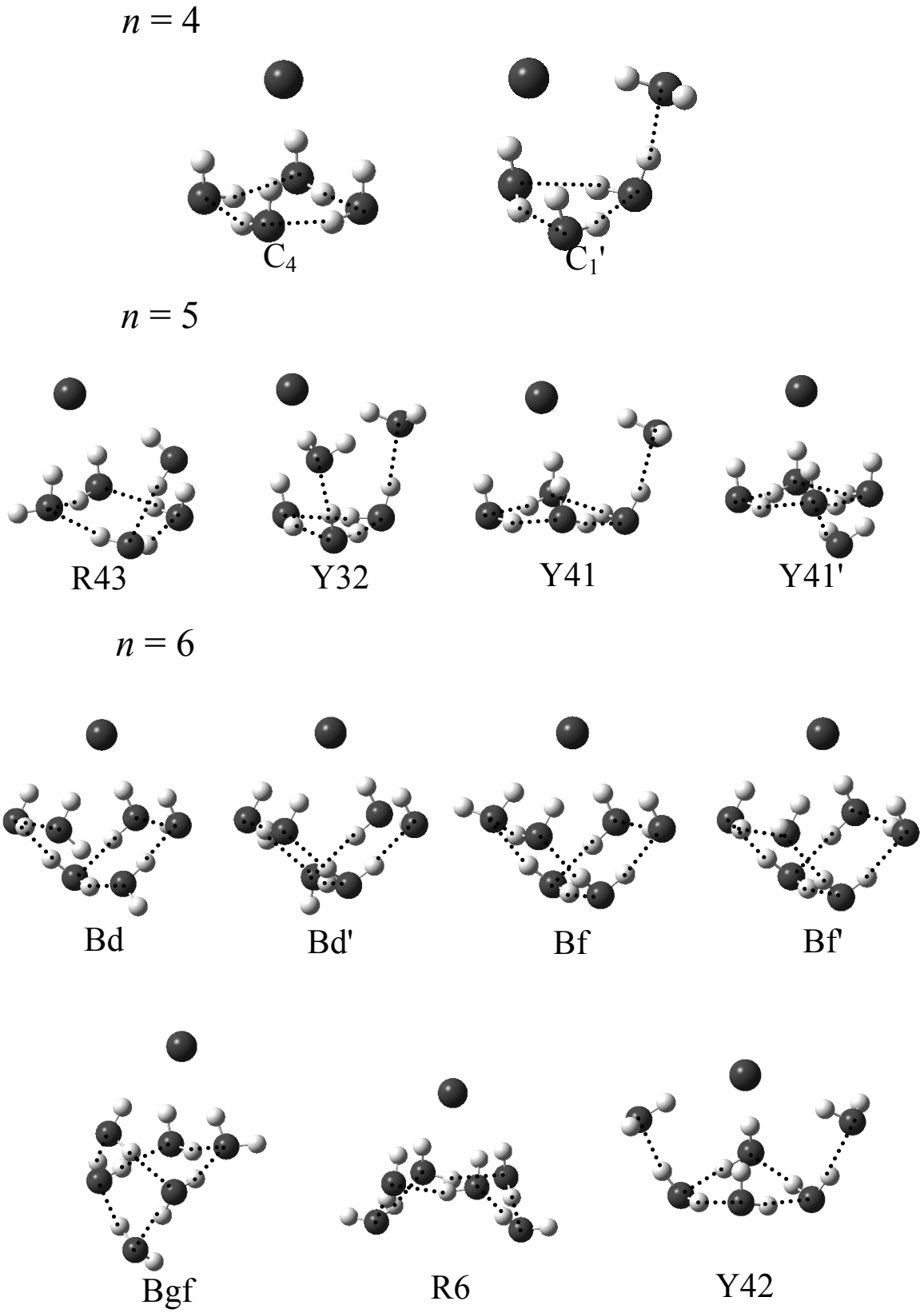

Fig. 1

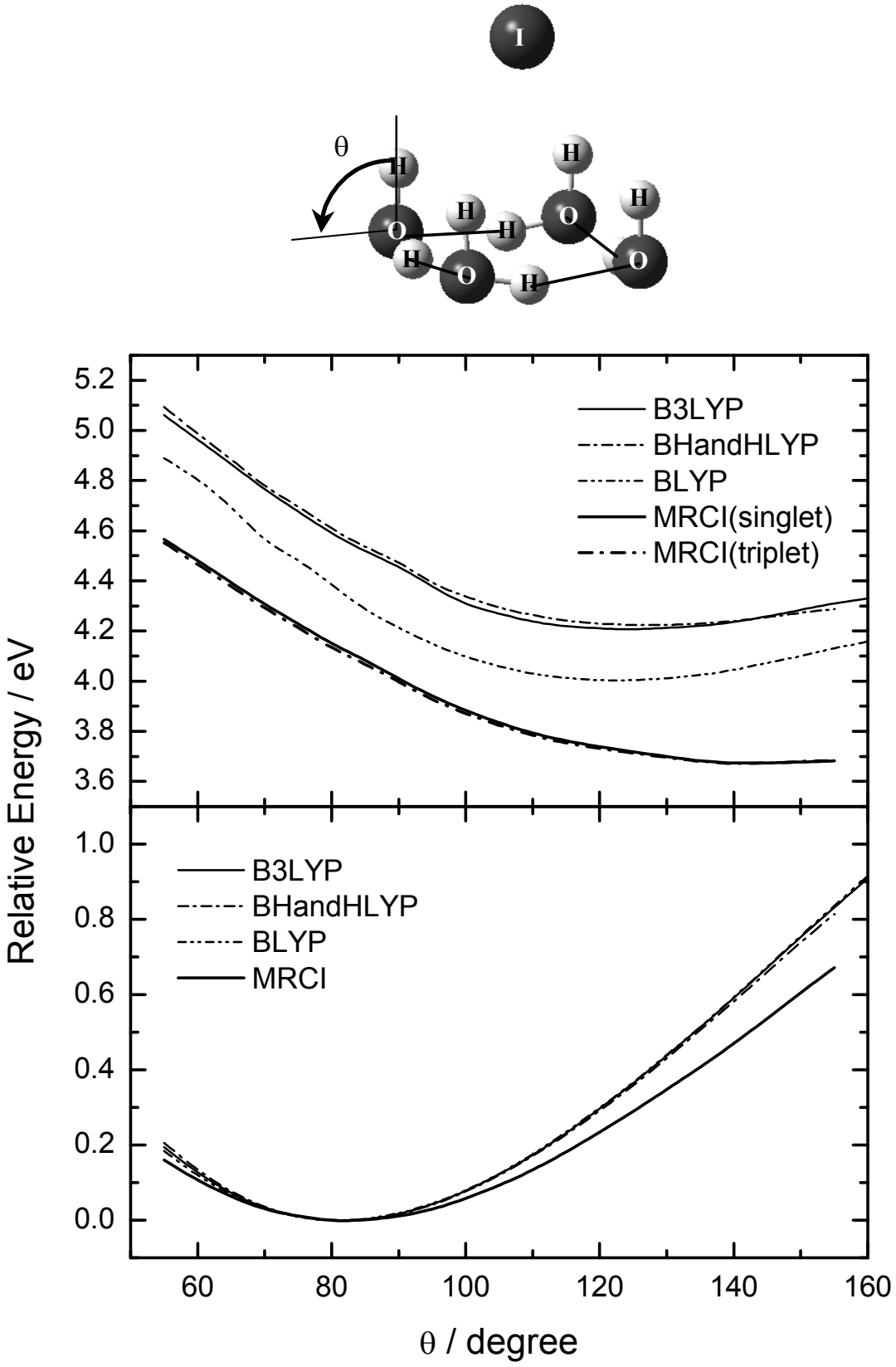
I
θ
H
O
5.2
5.0
4.8
4.6
4.4
4.2
4.0
3.8
3.6
B3LYP
BHandHLYP
BLYP
MRCI(singlet)
MRCI(triplet)
1.0
0.8
0.6
0.4
0.2
0.0
B3LYP
BHandHLYP
BLYP
MRCI
60
80
100
120
140
160
Relative Energy / eV
θ / degree

Fig. 2

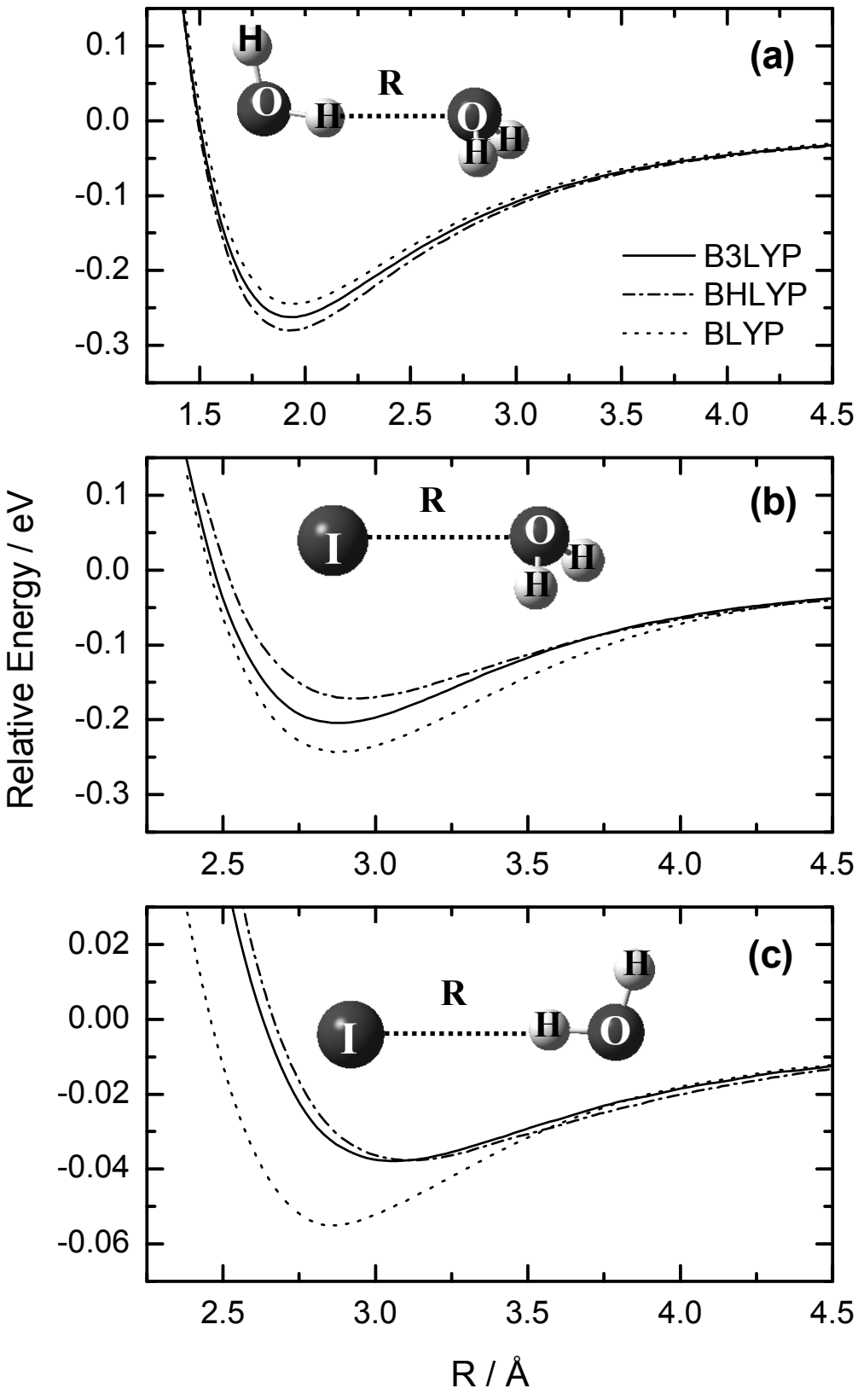

Fig. 3

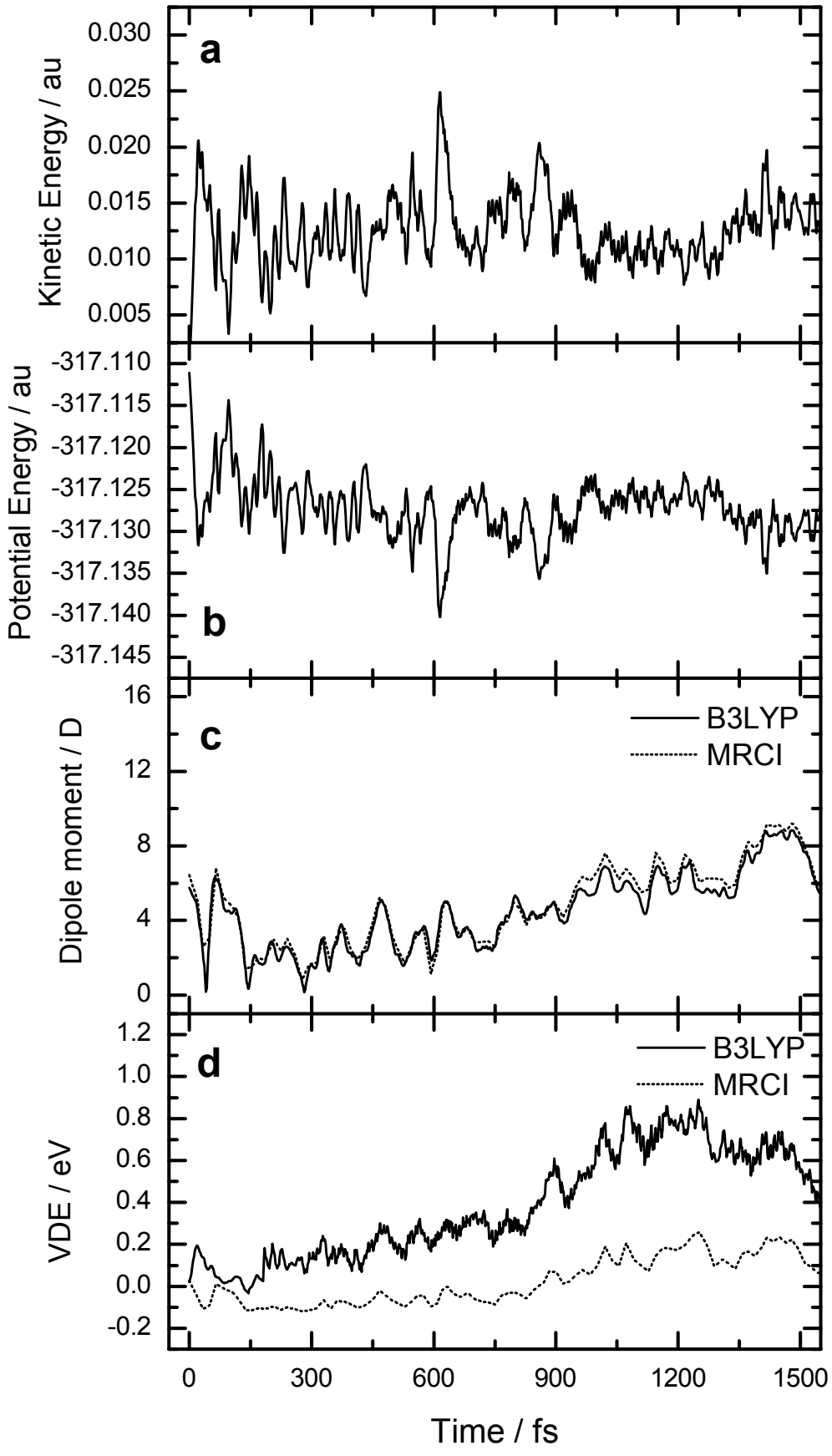
a
b
c
d
Kinetic Energy / au
Potential Energy / au
Dipole moment / D
VDE / eV
B3LYP
MRCI
B3LYP
MRCI
Time / fs
0.030
0.025
0.020
0.015
0.010
0.005
-317.110
-317.115
-317.120
-317.125
-317.130
-317.135
-317.140
-317.145
16
12
8
4
0
1.2
1.0
0.8
0.6
0.4
0.2
0.0
-0.2
0
300
600
900
1200
1500

Fig. 4

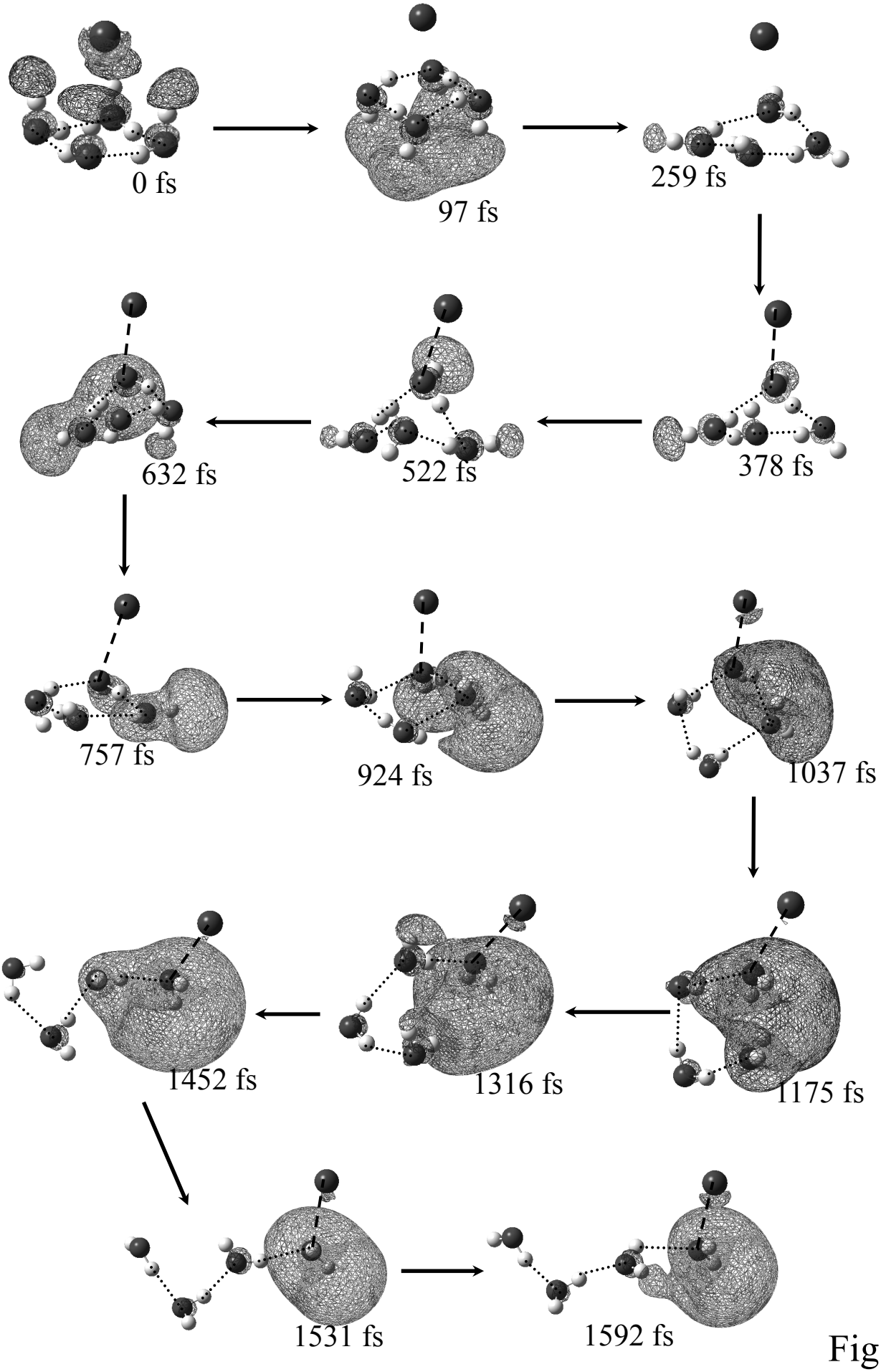
0 fs
97 fs
259 fs
378 fs
522 fs
632 fs
757 fs
924 fs
1037 fs
1175 fs
1316 fs
1452 fs
1531 fs
1592 fs

Fig. 5

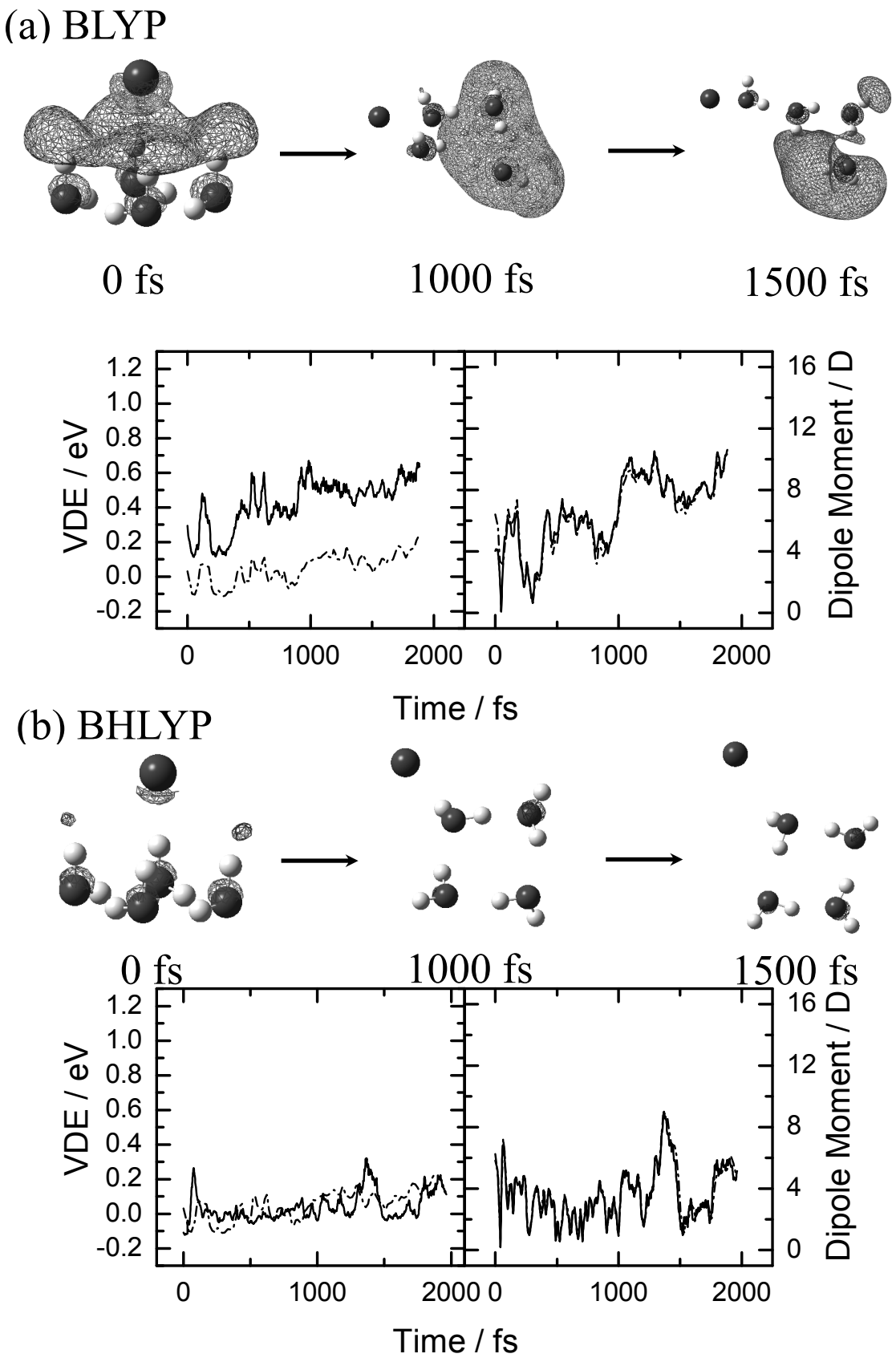
(a) BLYP
0 fs
1000 fs
1500 fs
VDE / eV
Dipole Moment / D
Time / fs
(b) BHLYP
0 fs
1000 fs
1500 fs
VDE / eV
Dipole Moment / D
Time / fs

Fig. 6

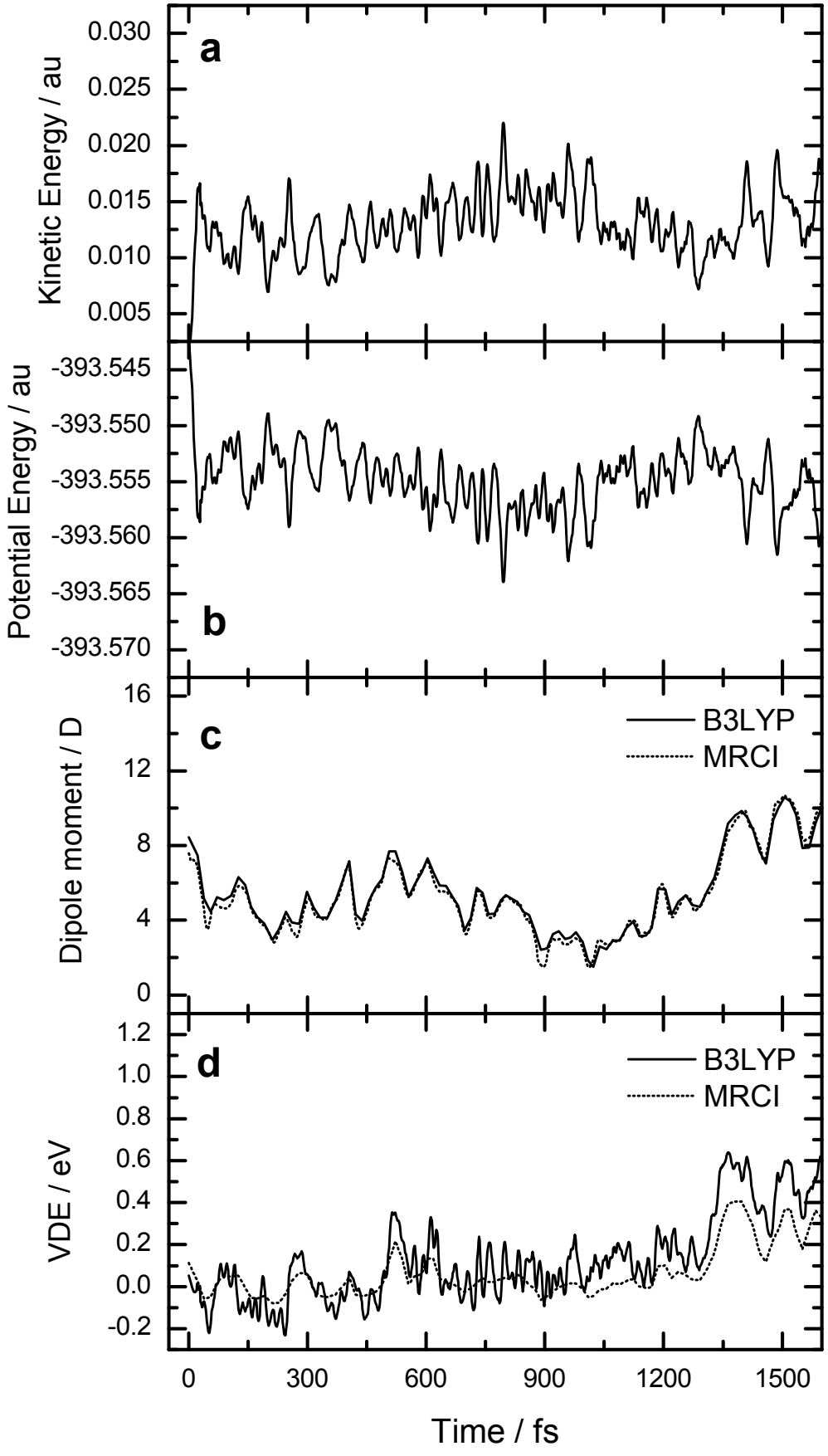
a
Kinetic Energy / au
0.030
0.025
0.020
0.015
0.010
0.005
b
Potential Energy / au
-393.545
-393.550
-393.555
-393.560
-393.565
-393.570
c
Dipole moment / D
16
12
8
4
0
B3LYP
MRCI
d
VDE / eV
1.2
1.0
0.8
0.6
0.4
0.2
0.0
-0.2
B3LYP
MRCI
0
300
600
900
1200
1500
Time / fs

Fig. 7

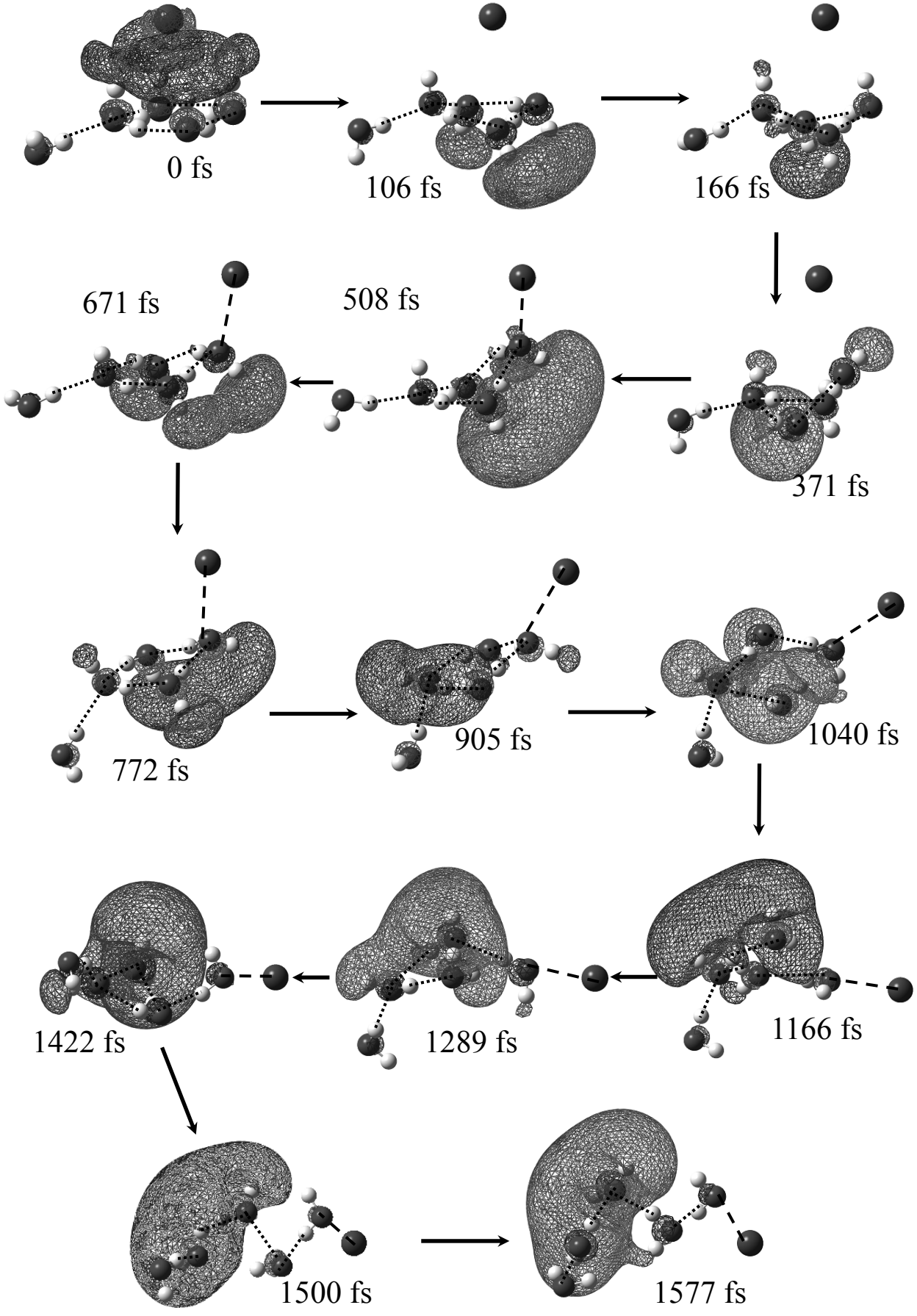
0 fs
106 fs
166 fs
371 fs
508 fs
671 fs
772 fs
905 fs
1040 fs
1166 fs
1289 fs
1422 fs
1500 fs
1577 fs

Fig. 8

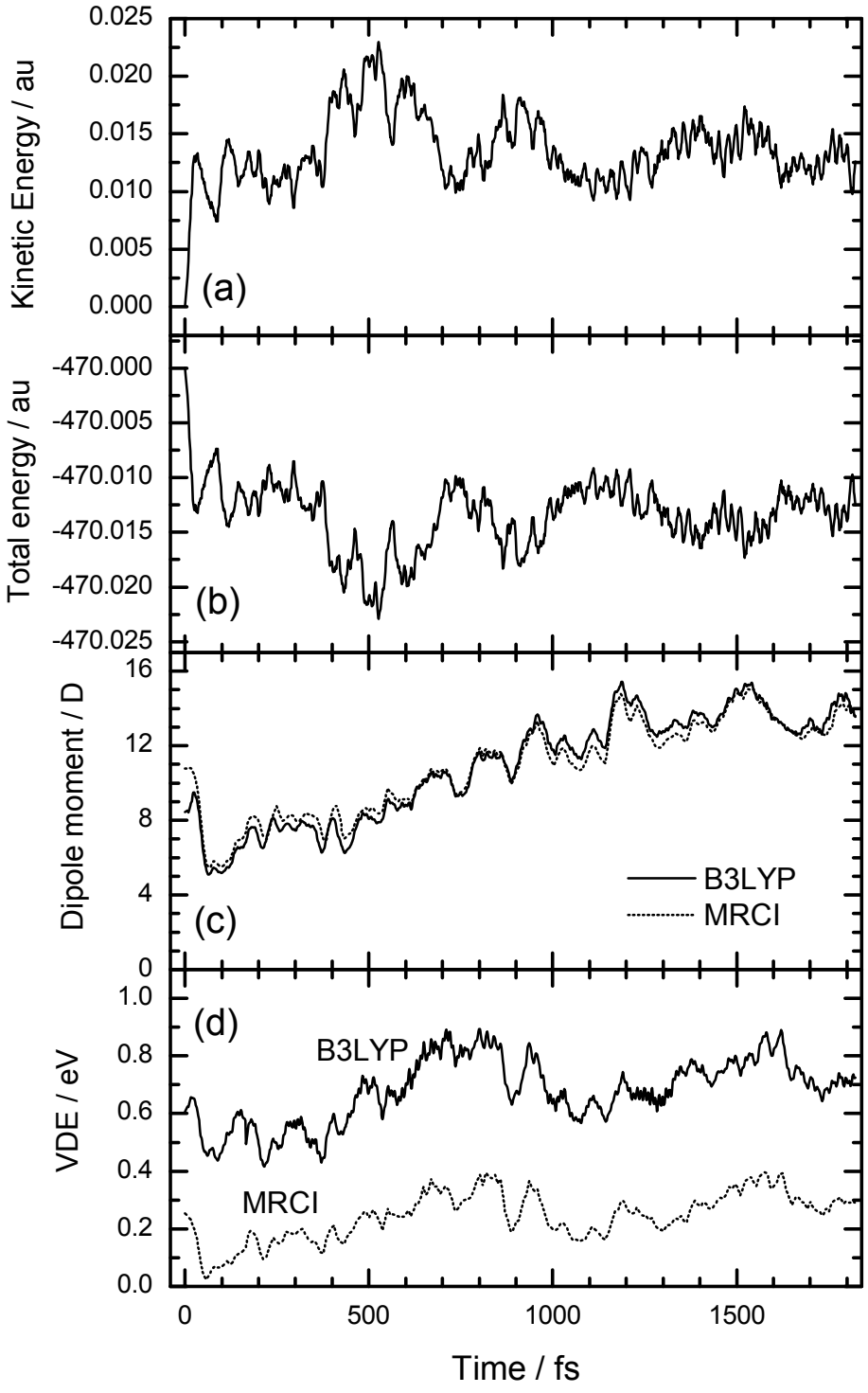
Kinetic Energy / au
0.025
0.020
0.015
0.010
0.005
0.000
(a)
Total energy / au
-470.000
-470.005
-470.010
-470.015
-470.020
-470.025
(b)
Dipole moment / D
16
12
8
4
0
(c)
B3LYP
MRCI
VDE / eV
1.0
0.8
0.6
0.4
0.2
0.0
(d)
B3LYP
MRCI
0
500
1000
1500
Time / fs

Fig. 9

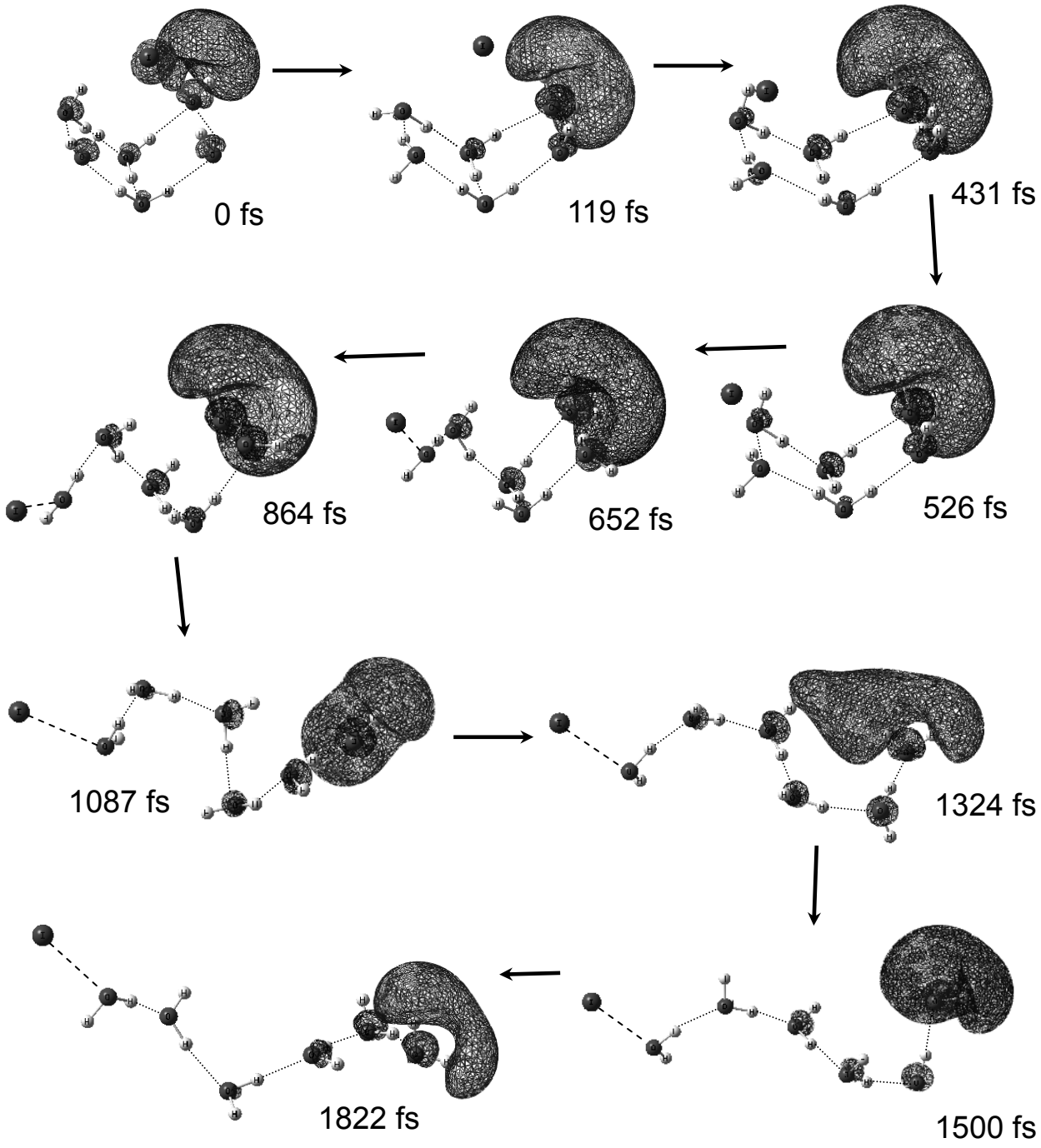
0 fs
119 fs
431 fs
526 fs
652 fs
864 fs
1087 fs
1324 fs
1500 fs
1822 fs

Fig.10

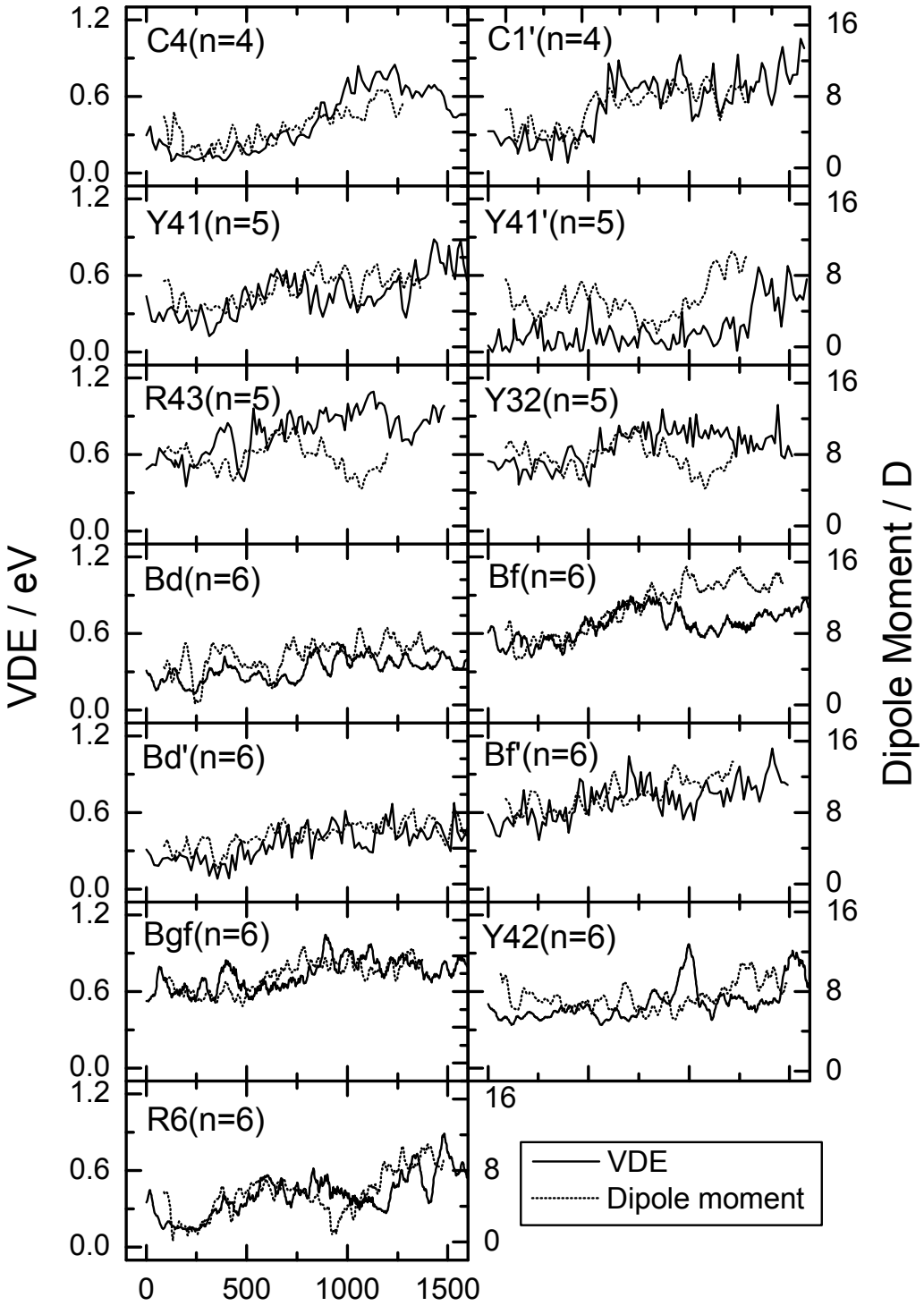
C4(n=4)
C1'(n=4)
Y41(n=5)
Y41'(n=5)
R43(n=5)
Y32(n=5)
Bd(n=6)
Bf(n=6)
Bd'(n=6)
Bf'(n=6)
Bgf(n=6)
Y42(n=6)
R6(n=6)
VDE / eV
Dipole Moment / D
VDE
Dipole moment
0
500
1000
1500

Fig.11